8

The Everett Integral and Its Analytical Approximation

Jenõ Takács
Department of Engineering Science, University of Oxford, Oxford UK

1.Introduction

The advancement in modern technology revolutionized our approach to the design of magnetic devices. The design requires concentrated effort from the designer to make the device more efficient. As a result, accurate modeling of magnetic materials in industrial application becomes a vital part of the design procedure. Amongst the number of hysteretic models for magnetic substances available for the user, the best known and commonly used is still the geometrical model suggested by Ferenc Preisach in 1935 (Preisach, 1935). Although various authors suggested a number of modifications for different applications, (Della Torre, 1999; Mayergoyz, 2003) somehow in various forms it still survives as the dominating hysteresis model of our time. The modified versions include the classical, static, dynamic, state-independent, state dependent, reversible, and vector, etc. Detailed discussion of the model can be found in the literature, for instance by Mayergoyz, Bertotti and Della Torre (Bertotti, 1998; Della Torre, 1999; Mayergoyz, 2003).

The principal assumption of this model, is that any magnetic material is a composition of basic particles called hysterons with the characteristic switching up U and switching down V magnetic field values, with a characteristic square like hysteresis loop. Hysterons are elementary hysteresis loops or hysteresis operators characterized by the switching fields.

Fig.1 Shows two hysterons displaced by H_s in the magnetic domain, schematically.

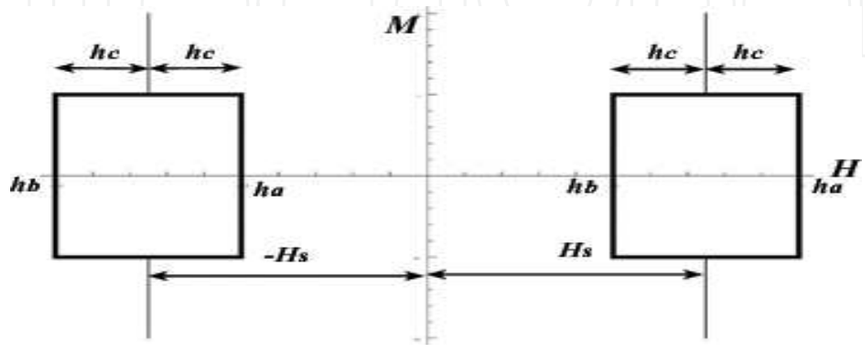

Fig. 1. Schematic representation of two elementary hysteresis operators or hysterons, displaced by H_s to the negative and the positive direction.

These hysterons, in Fig 1, populate the hysteresis loop in a statistical manner, whose distribution density is described mathematically by the Preisach function (Ivanyi, 1997; Della Torre, 1999; Mayergoyz, 2003). In the classical Preisach scalar model (CPSM) this leads to the magnetisation expression versus time in the following form , known as Everett integral (Mayergoyz, 2003).

$$M(t) = \iint_{T} P(U,V)dUdV - \iint_{-T} P(U,V)dUdV \tag{1}$$

Here, *M(t)* is the sum of the magnetisation of the hysterons and *T* and *–T* are the positive and negative domains of the Preisach triangle, where hysterons contribute positively or negatively to the overall time dependent magnetisation (Kadar et al, 1989). Fig. 2 shows the Preisach triangle in the plane of the switching field.

In Preisach based models the fundamental difficulty is the determination of the *P(U,V)* distribution function, which is called in general terms as "the identification problem" (Mayergoyz, 2003; Ivanyi, 1997) determined by the set of the symmetrical first order reversal loops. To solve the problem of so called "identification", some authors suggested substituting the Preisach distribution function with suitable approximations. Mayergoyz suggested power series (Mayegoys et al., 1990), while Kadar and Della Torre used the bilinear product of Gaussian functions (Kadar & Della Torre, 1988) for the solution of the Everett integral (1).

In spite of the large variation of modified Preisach models all variants have failed to model the complicated variety of hysteresis loops, such as the spin valve and anti-spin valve configurations (see Section 9). The only successful approach so far was, to our knowledge, the hyperbolic analytical approximation, in that field.

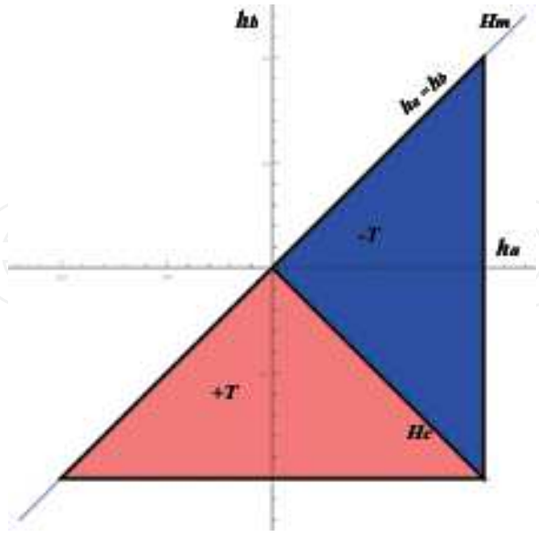

Fig. 2. The Preisach triangle in the plane of switching field.

Here h_a and h_b are the normalised switching fields (for normalization see Section 10) and *Hc* is the coercivity.

For soft materials, where the Gaussian approach failed to provide acceptable results, Finocchio and his co-workers suggested Lorentzian distribution (Finocchio et al., 2006). All approximations have their positive and negative sides and can only be used for certain type of materials.

The two latest approximations will allow analytical evaluation of the Everett integral in closed mathematical terms.

Takacs in his paper published in 2000 introduced the hyperbolic distribution (Takacs, 2000) to approximate the sigmoid- like hysteresis loops and to mathematically describe the different properties of various magnetic substances. At the time this model, based on Langevin's theory (Bertotti, 1998), was purely phenomenological and no connection was assumed to the Preisach classical approach.

The hyperbolic distribution *T(x)* can be described mathematically in its simplest form as

$$T(x) = A\ \mathbf{sech}^2\alpha(x-a) \tag{2}$$

Here A represents the amplitude, a is the shift in position of the function and α controls the steepness of the curve. A typical hyperbolic and a Gaussian distribution are shown in Fig 3. As we can see from the graphs, the hyperbolic distribution is running very close to the Gaussian line in spite of having quite different mathematical properties. The close relation between the two models (classical Preisach and hyperbolic) was only discovered recently and published here for the first time.

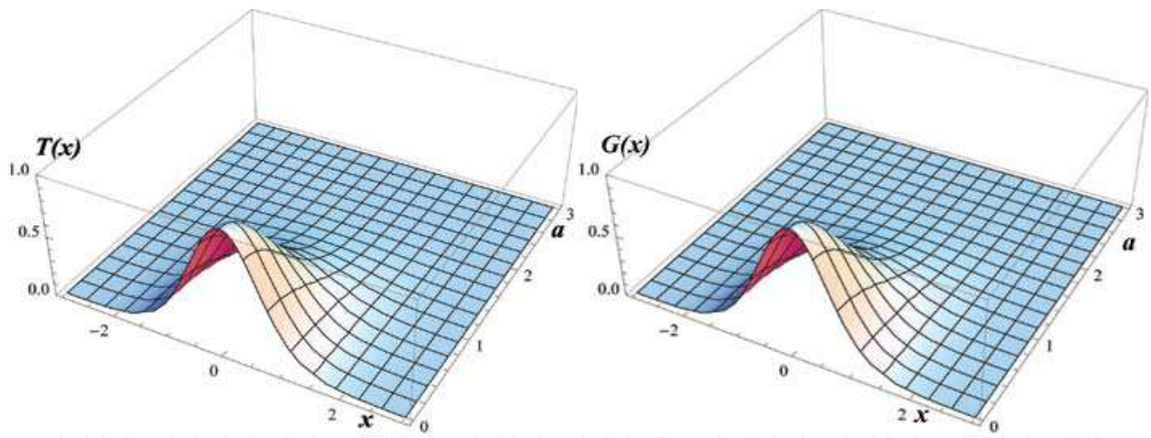

(a) (b)

Fig. 3. Distribution functions: (a) hysteretic, (b) Gaussian.

Bertotti pointed out (for details see (Bertotti, 1998)), that in most cases, the Everett integral in (1), particularly for symmetrical loops, can be replaced finally with a function of a single running variable, representing the excitation field *H*. In this argument we always assumed, point symmetry in the system, therefore

$$T(H - H_c) = T(H + H_c) \tag{3}$$

There is particular interest in functions, where the distribution can be formed as the product of two terms in the form of

$$T(H,H_c) = T(h_a)T(h_b) = T(H+H_c)T(H-H_c) \tag{4}$$

where h_a and h_b are the switching fields (see Fig. 2)

Using the hyperbolic distribution, shown in (2) substituted into (1), the Everett double integral will take the following form:

$$M(t) = \iint_{T} T(H,H_c)\gamma(H,H_c)dHdH_c - \iint_{-T} T(H,H_c)\gamma(H,H_c)dHdH_c \tag{5}$$

where
$$\gamma(H,H_c) = \begin{cases} +1 \textbf{ if } (H,H_c) \in +T \\ -1 \textbf{ if } (H,H_c) \in -T \end{cases}. \tag{6}$$

When
$$T(H,H_c) = A\textbf{sech}^2[\alpha(H-H_c)]\textbf{sech}^2[\alpha(H+H_c)] \tag{7}$$

By substituting (7) and (6) into (5) we obtain (Kadar et al., 1987 and 1988)

$$M(t) = \iint_{T} T(H,H_c)dHdH_c - \iint_{-T} T(H,-H_c)dHdH_c \tag{8}$$

A Preisach elementary operator, populating the Preisach plane with the hyperbolic character is shown in Fig. 4. We can now solve Everett's integral in (8), by using hyperbolic distribution in (2), leading to the following expressions for the ascending and descending magnetization correspondingly:

$$M_u = A\ tanh[\alpha(H-H_c)] + F(H_{\mathrm{m}}) \tag{9}$$

$$M_d = A\ tanh[\alpha(H+H_c)] - F(H_{\mathrm{m}}) \tag{10}$$

Here A represents the maximum amplitude of the magnetization, H_c is the coercivity, H_m is the maximum excitation, α is the differential permeability at $H = H_c$ or the angle of the tangent of the hysteresis loop at the point where it crosses the field axis. The F integration constant can be calculated from the condition, that at the first return point, where M_u and M_d must be equal, for all minor and major loops (Della Torre, 1999; Mayergoyz at al.,1990), therefore per definition:

$$F(H_{\mathrm{m}}) = \frac{A}{2}[\tanh\alpha(H_m + H_c) - \tanh\alpha(H_{\mathrm{m}} - H_c)] \tag{11}$$

The capital letters represent the physical quantities and the corresponding lower case letters will refer to the normalized units. The normalization used in this chapter is not related necessarily to the maximum value. It is the free choice of the user; the base can be any convenient number, which helps to carry out the mathematical operations. A long detailed description of the free normalization process can be found in Section 10.

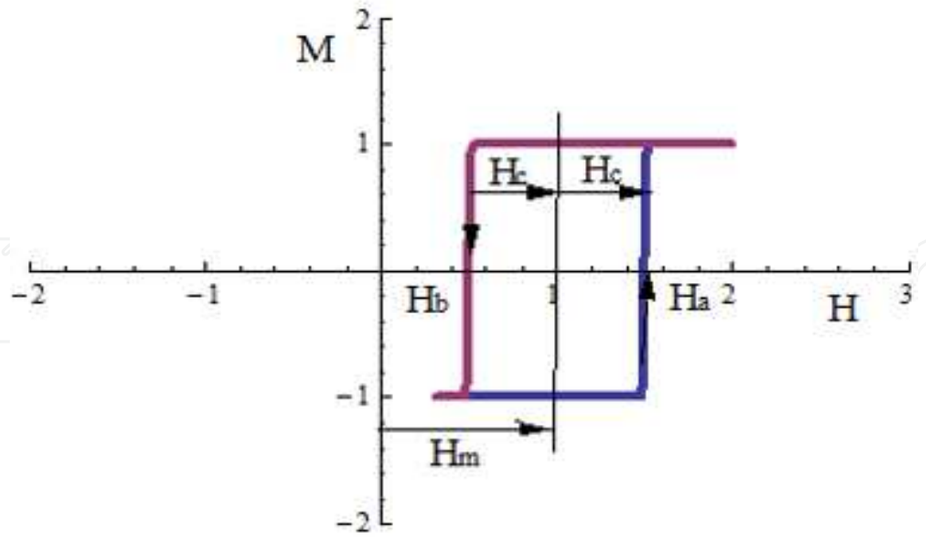

Fig. 4. Preisach elementary operator (hysteron) with hyperbolic character.

After normalization the ascending m_u and the descending m_d branches of the hysteresis loop can be written as:

$$m_u = a\ tanh[\alpha(h - h_c)] + f_0 \tag{12}$$

$$m_d = a\ tanh[\alpha(h + h_c)] - f_0 \tag{13}$$

respectively, where

$$f_0 = \frac{a}{2}((\tanh[\alpha(h_{\mathrm{m}} + h_c)] - (\tanh[\alpha(h_{\mathrm{m}} - h_c)]) \text{ is the normalized form of } F(H_m) \tag{14}$$

Here, all lower case letters represent the appropriate normalized quantities. In this study, where-ever possible, the normalized form is going to be used.

2. Fundamentals of the hyperbolic model

The hyperbolic model analytical approach is based on the practical assumption, that in general, there are at least, three parallel processes, including very soft irons, dominating the overall magnetization process; i.e. the reversible and irreversible domain wall movement (DWM), the reversible and irreversible domain rotation (DR) and the domain wall annihilation and nucleation (DWAN) processes (Varga at al., 2008). Although these processes are interlinked, they can be mathematically formulated separately and combined, by using Maxwell's superposition principle. They individually dominate the low, middle and near saturated region of magnetization and are supposed to have also have sigmoid shapes. This model is already used successfully in number of applications (Takacs at al, 2008; Nemcsics at al., 2011; Jedlicska at al., 2010) and some aspects are already well documented in the literature (Takacs, 2003).

When numerous processes are running simultaneously, it is difficult to describe the overall magnetization with one function, resulting from the integration of one Everett integral, but the combination of all the concurrent processes brings the model nearer to the experimental results (Takacs, 2006; 2008). The magnetization processes of magnetic materials, particularly for ultrasoft substances and the role of the domain rotation (DR) and domain wall movement (DWM) in the process has been the subject of recent experimental and theoretical studies. Fitting the experimentally obtained curves with analytical expressions of the hyperbolic model, provided a useful tool for obtaining the mixed second derivative of the curves, eliminating the deviation, between the model and the experimental data. The diagram of mixed second derivatives, as conceived by Pike (Pike et al., 1999) can be obtained for both the set of first order reversal curves (FORC diagram) and for the set of biased first magnetization curves (BFMC diagram), respectively. These FORC and BFMC diagrams of any magnetic system can be measured and modelled irrespective of their magnetic softness/hardness. It was assumed that all processes have hyperbolic (sigmoid) character, but they differ in the model parameters including the (near) reversible part as suggested by Della Torre (Della Torre, 1999; Jiles et al. 1983). All these components can be formulated mathematically as:

$$m_u = \sum_{k=1}^{n} [a_k f_{uk} + f_{0k}(h_{\mathrm{m}})] \tag{15}$$

$$m_d = \sum_{k=1}^{n} [a_k f_{dk} - f_{0k}(h_{\mathrm{m}})] \tag{16}$$

$$f_{uk,dk} = \tanh[\alpha_k (h \mp h_{ck}) \tag{17}$$

Where n is the total number of processes present and k is the running variable. Normally n is running between 1 and 3.

Fig. 5 demonstrates a typical application of the hysteresis model. Fig. 5 a. shows the major hysteresis loop of a toroid made of NO Fe-Si and Fig.5 b depicts the three constituent components. For fitting the measured loop (broken line), in Fig. 5 a, we used equations (15), (16) and (17), with the following normalised and physical parameter values.

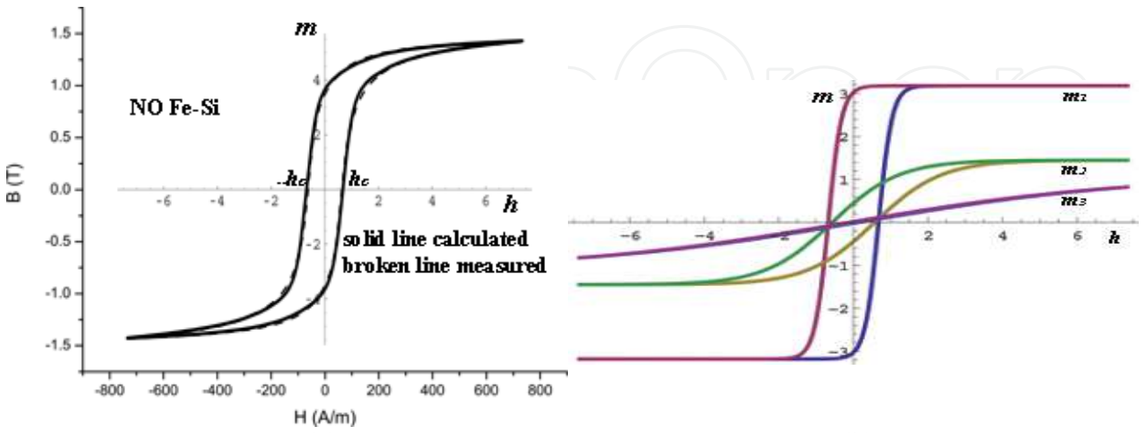

(a) (b)

Fig. 5. Measured and calculated major hysteresis loop of NO Fe-Si toroid, measured broken line, calculated solid line. The components are drawn in different colours.

$a_1 = 3.18$, $a_2 = 1.45$, $a_3 = 1.09$,
$\alpha_1 = 2.75$, $\alpha_2 = 0.56$, $\alpha_3 = 0.134$
$h_{c1} = 0.675$, $h_{c2} = 0.57$, $h_{c3} = 0.2$, $h_m = 7.35$
Corresponding to: $A_1 = 0{,}842$ T, $A_2 = 0.384$ T, $A_3 = 0.288$ T
$H_{c1} = 67.5$ A/m, $H_{c2} = 57$ A/m, $H_{c3} = 20$ A/m, $H_m = 57$ A/m

with free (arbitrary) normalization (see Section 10) of 1 h = 100 A/m for the field and 1 m = 0.53 T for the magnetization.

The normalization factors can be read from the two coordinate systems (normalized in the middle and outside one measured). For detailed explanation for the normalisation process see Section 10.

The other well-known hysteresis model, based on Lagevin function is the Jiles-Atherton model (Jiles, 1994). This model fundamentally considers, as its principle, the interaction between domains and already includes the internal demagnetisation in the form of the Weiss field (see Section 4); therefore it falls into the category of dynamic models. Its five parameters however are often difficult to associate with parameters used in practical magnetism. While in the hyperbolic model the number of parameters is the choice of the user and can vary between three and nine (depending on the accuracy required), in the J-A model this number is fixed. In complex cases the set parameters are not enough to model the phenomenon, therefore for a number of applications the model had to be modified for the specific purpose (Carpenter, 1991; Carpenter et al. 1992; Korman et al. 1994). In the iteration process, to obtain the model parameters, there is very little difference between the models of hysteresis but the hyperbolic model with its utmost simplicity provides a clear and practical method for the practical user. In the following a number of useful examples will illustrate possible applications of the model for the potential user.

3. Symmetrical and biased major and minor loops

Modeling of a regular shape hysteresis loop is based on the functions defined in (9) and (10). By using functions, mimicking the sigmoid shape of the hysteresis loop, one can formulate both phenomena of saturation and hysteresis. Changing h_m between zero and saturation field values, with a slow changing ac field we can obtain a set of minor and major loops for a given set of a, α, h_c and h_m (amplitude, differential susceptibility, coercivity, maximum magnetization) values. The substitution of these values into (15), (16) and (17) will give the solution of the Everett integral for every loop, minor or major in the set. At steady state, the first return points will sit on the theoretical or intrinsic loci, the only theoretical line, which belongs to both the ascending and the descending set of branches. It is un-hysteretic, but carries all the properties of the hysteresis loop. Due to the ever present internal demagnetization, it is an entirely theoretical concept. It cannot be realized experimentally, (internal demagnetization cannot be reduced to zero), nevertheless both f_0 and m_0 secondary functions will help in later calculations (see Part 6). By definition m_0 can be formulated as:

$$m_0 = (m_u + m_d)/2 = \frac{a}{2}(\tanh[\alpha(h + h_c)] + \tanh[\alpha(h - h_c)]) \tag{18}$$

For the definition of f_0 see (14).

Fig. 6a shows a set of symmetrical major and minor loops, calculated from (15), (16) and (17).

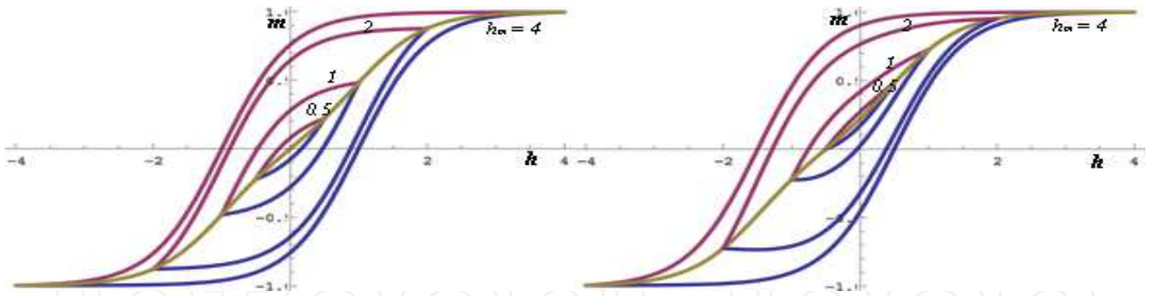

(a) (b)

Fig. 6. (a) and (b) show typical symmetric and biased major and minor loops.

In practice very often, like in power transformers, dc current is passing through the windings creating a constant dc field with the ac superimposed on it. This represents a shift in the first reverse points in the direction of the bias. The solution of the integral for the biased hysteresis loops is shown in (19), (20) and (21). For the detailed explanation the reader is referred to Ref. (Takacs, 2003).

Let us assume the dc field represents a normalize b bias on the magnetic object. This increases the effect of the magnetizing field in the following way:

$$m_u = a\ \tanh[\alpha(h - h_c + b)] + f_{00} \tag{19}$$

$$m_d = a\ \tanh[\alpha(h + h_c + b)] - f_{00} \tag{20}$$

$$m_0 = a\ \{\tanh[\alpha(h + h_c + b)] + \tanh[\alpha(h - h_c + b)]\} / 2 \tag{21}$$

where by using laws of a line going through two point in the hyperbolic domain.

$$f_{00} = f_1 \frac{m_0(-x_m) - m_0(x)}{m_0(-x_m) - m_0(x_m)} + f_2 \frac{m_0(x_m) - m_0(x)}{m_0(x_m) - m_0(-x_m)} \tag{22}$$

$$f_1 = \{tanh[\alpha(-h_m + h_c + b)] - tanh[\alpha(-h_m - h_c + b)]\} a / 2 \tag{23}$$

$$f_2 = \{tanh[\alpha(h_m + h_c + b)] - tanh[\alpha(h_m - h_c + b)]\} a / 2 \tag{24}$$

where b represents the bias applied, in normalized form.

4. Experimental loci of the first return points

The prime aim of most magnetic measurement is to find the intrinsic magnetic properties of the tested material. Due to the ever presence of the demagnetization field, (Fiorillo, 2004) a number of measuring methods have been developed to minimize its effect. The most commonly accepted way is to make the sample into a closed magnetic circuit, like a toroid or an Epstein square (Korman et al. 1994; Fiorillo, 2004). Although these two are not completely free from the presence of the internal demagnetization, they suffer the least from it. Authors went into great length to include the internal demagnetization force into the known models like Preisach, Stoner-Wohlfarth, Jiles (Preisach, 1935; Stoner et al. 1991; Jiles, 1996) etc. leading to so called, dynamic versions.

Within the saturation loop lie the loci of the vertices (first return points) of the symmetrical minor loops, which is when measured, differs from that of the theoretical intrinsic line calculated from saturated hyteresis loop data, free from internal demagnetization (i.e. Classical Preisach, hyperbolic model, etc). The relationship between the two curves can be formulated in closed mathematical form, independent of any models. To describe the internal demagnetising field, we can use the concept of the effective field, analogous to the Weiss mean field, used by other authors also (Jiles 1998; Barkhausen, 1919; Alessandro et al. 1990). Generally the H_d demagnetizing field vector is antiparallel to M vector and proportionality is assumed between H_D interaction field and M magnetization. This accepted linear approximation is

$$H_{eff} = H + N_d M \tag{25}$$

where, by using Jiles notations N_d is the internal demagnetization factor.

The internal demagnetization factor N_d usually given in tables with unity dimension. We must remember that its numerical value and dimension depends on the units used. This dimension is only unity, when both M and H_D measured in ampere per meter. When other unit convention is used, then N_d –s dimension is not unity and must be normalised like other magnetic quantities.

In normalised form with the normalised magnetization with effective field is

$$f(h_{eff}) = f(h + n_d m) \tag{26}$$

where f function is the analytical approximation of the integrated Preisach function. After substitution of (26) into the expression of the intrinsic loci we arrive to a model free expression of m_0 of the following form:

$$m_0 = f(h + n_d m_0) \tag{27}$$

The first derivative of m_0 by h of equation in (27) leads to an expression, which shows a character, similar to the feedback in an electrical circuit (Fiorillo, 2004; Jiles, et al.1986).

$$\frac{dm_0}{dh} = \frac{\frac{dm_0}{dh_{eff}}}{1 - n_d \frac{dm_0}{dh_{eff}}} \tag{28}$$

Expression (28) describes the relationship between the inherent (χ_{in}) and the effective (χ_{eff}) susceptibility (Fiorillo, 2004; Jiles, 1998). Here the inherent susceptibility is a material property, while the effective one is measured and depends on the geometry of the sample and the air gap included in the magnetic circuit, used in the measuring setup.

For most magnetic substances the value of N_d is small in the order of -10^{-5} when given in unity dimension (Jiles, 1998). Expansion of (28) into its geometric progression (Tranter, 1971), truncated at three terms ($n = 3$) will yield the following expression:

$$\frac{dm_0}{dh} = \frac{dm_0}{dh_{eff}}(1 + n_d \frac{dm_0}{dh_{eff}} + (n_d \frac{dm_0}{dh_{eff}})^2 + ...) \tag{29}$$

The first term in equation (29) depends on the intrinsic (N_d = *0,* see Part 6) material parameters only.

Following the integration of expression in (29) by h_{eff} will lead us to the measured loci m_0. (We assume n_d is small and $dh \approx dh_{eff}$). When the integration, carried out by using generalized integration by parts (Tranter, 1971) we arrive at the following expression.

$$m_0(h) \approx m_{01}(1 + n_d \frac{dm_{01}}{dh} + \ (n_d \frac{dm_{01}}{dh})^2 + ...) \tag{30}$$

Here $m_{01,}$ for $n_d = 0$ is representing the intrinsic or theoretical loci of the vertices (the same theoretical concept is used at the free energy calculation in Section 6). With the appropriately selected n_d in most practical cases the first two or three terms gives good enough accuracy in calculation. Fig. 7 depicts a measured, intrinsic and a calculated curve using (30). Fig.8 shows one measured minor loop and its equivalent, modelled with expression in (30).

We can conclude from (30) that the losses due to the internal demagnetization are proportional to the Preisach function in first approximation.

Based on experimental evidence, N_D (not normalised) can be approximated as

$$N_D \approx \mu_0 \frac{H_c}{B_s} \tag{31}$$

where B_s is the saturation induction.

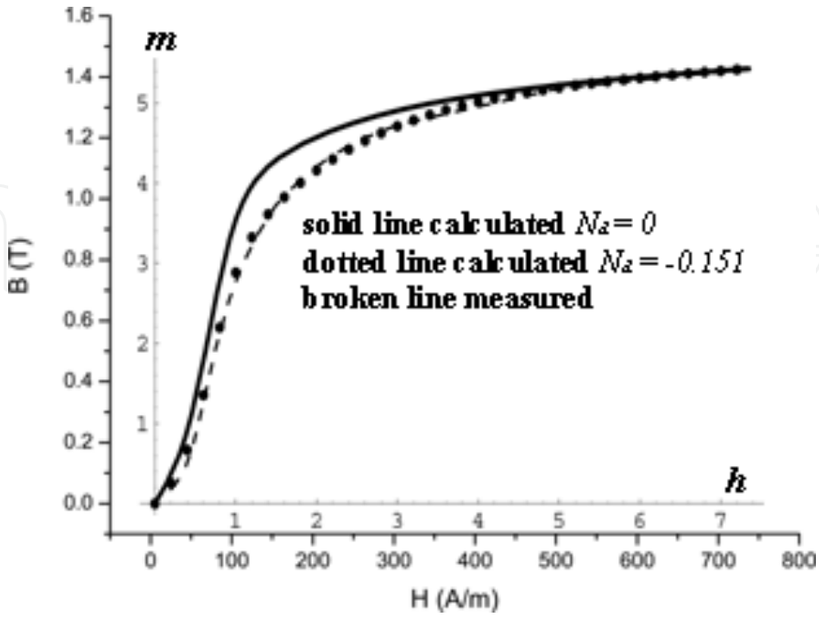

Fig. 7. Measured (broken line), modelled (dotted line) and intrinsic (solid line) loci for NO Fe-Si

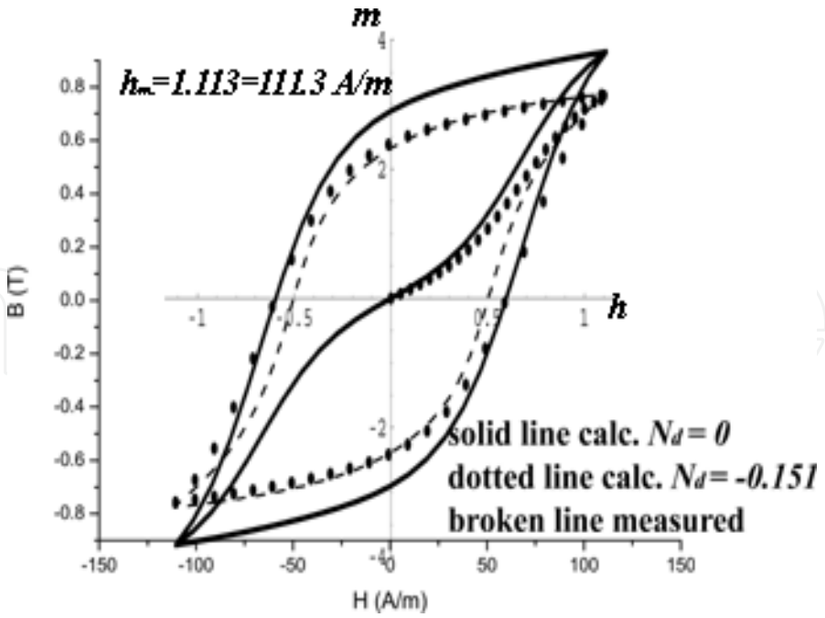

Fig. 8. Calculated NO Fe-Si minor hysteresis loop for N_d = 0 (solid line) and N_d = – 0.151 (dotted line), fitted to the measured loop (broken line) with internal demagnetization.

5. Hysteresis loss and stored energy

In ac applications one of the vital properties of the magnetic material is its electrical loss. This represents the energy dissipated by the device as heat. The hysteresis loss is shown to be proportional to the area enclosed inside the hysteresis loop (Steinmetz, 1891). As an indicator, it is the measure of the loss per unit volume over one cycle of the periodic excitation (Steinmetz, 1892). While the other losses (eddy current, excess etc.) depend on the geometry of the sample, frequency, conductivity and other parameters, (Bertotti, 1998) the hysteresis loss is related primarily to the area enclosed by the hysteresis loop. We intend to formulate this enclosed area, therefore show an analytical way to calculate the hysteresis loss in magnetic substances.

The total area T (not to be taken as the Preisach triangle or Tesla) inside the hysteresis loop is represented by the difference between the integrals of the m_u and m_d functions in (12) and (13) by h, between the limits of $\pm h_m$ maximum field excitations, in the following way:

$$T = \int_{-hm}^{hm} a\,(\tanh[\alpha(h+h_c)] - f_0)dh - \int_{-hm}^{hm} a\,(\tanh[\alpha(h-h_c)] + f_0)dh \tag{32}$$

The final result of this integration is shown in equation (33) for n number of components.

$$T = \sum_{k=0}^{n} \{2\frac{a_k}{\alpha_k}[\ln\cosh\alpha_k(h_m - h_{0k}) - \ln\cosh\alpha_k(h_m + h_{0k})] - 2f_k h_m\} \tag{33}$$

It is customary after Steinmetz, to plot the losses proportional to the area as the function of the maximum magnetization. Fig.9 shows the losses versus h_m. The graph depicts also the

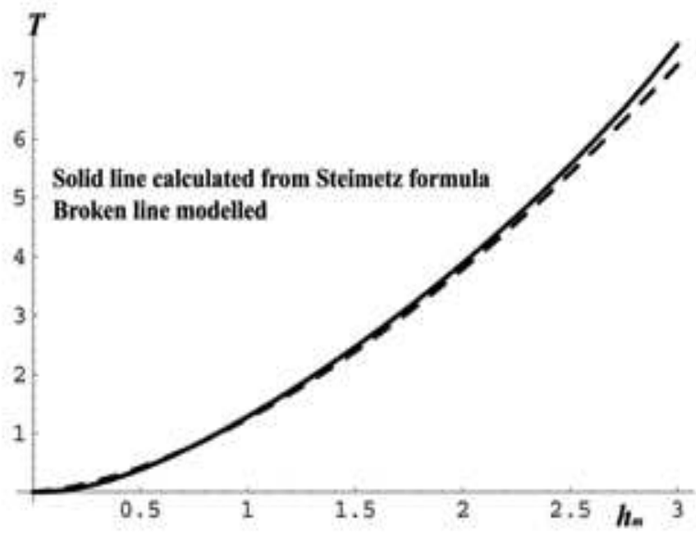

Fig. 9. The T area, (proportional to the hysteresis loss) versus h_m and its Steinmetz' approximation.

$Kh_m^{1.6}$ curve, or Steinmetz's approximation. It shows that for soft steel, with coercivity around 70 A/m, the Steinmetz approximation is within a few per cent to the theoretical value, up to near saturation for the materials constant $K = 1.25$, which is very close to 1.1 value, predicted by the model.

For permanent magnet manufacturers one of the most important parameters is the maximum energy product. It is a measure of the total energy that can be produced by the magnet, or the maximum amount of work, that the magnet can do outside the volume of the magnet. When it is related to its volume, we come to the energy product density, which by nature is independent of the geometry of the magnet; therefore it is entirely a material parameter.

For a permanent magnet the integral of the field - induction product for the whole space must be zero as there is no external energy introduced to the closed system (Jiles, 1998). The system is in an equilibrium state. The total energy can be divided in to the energy inside the volume of the magnet ν and the energy outside. It is self-explanatory therefore, from (34) that the two energies inside and outside of the magnet must be equal.

$$\int^{space} HB\, dv = \int^{inside} HB\, dv + \int^{outside} HB\, dv = 0 \tag{34}$$

Outside of the magnet $B = \mu_0 H$ therefore we can write the following equation

$$\int^{inside} \mu_0 H^2\, dv = \int^{outside} HB\, dv \tag{35}$$

We can say that the energy of the field H outside the magnet is equal to the HB product inside the magnet integrated over the whole volume of the magnet. The geometry of a magnet is normally well defined, therefore it is enough to calculate the energy stored in a unity volume called the "energy density". The energy density w stored in a medium permeated by a magnetic field can be expressed as

$$w = \int_0^B H \, dB = HB - \int_0^H B \, dH \tag{36}$$

Let us use Preisach function and substitute it into (34). This substitution will yield the following:

$$w = \int h \, [a\alpha \, \mathbf{sech}\alpha(h + h_0)]^2 \, dh \tag{37}$$

A simple but representative quantity for the energy stored, often used in practice (Jiles, 1998), is the product of the magnetic induction and the magnetic field per unit volume. The larger the $(HB)_{\max}$ product for a magnetic material the better are the magnetic properties of a permanent magnet. Expressing h from (13) the energy product hb (the normalised HB product) can be described as

$$hb = \mu_0 m_d h = \frac{m_d}{\alpha} \mathbf{arctanh} \left(\frac{\mu_0 m_d + f_0}{a} \right) - h_c m_d \tag{38}$$

According to an accepted custom, it is usually shown as a function of the magnetic induction. Fig. 10 shows a typical schematic hb curve as a function of m_d with its maximum around m_d = 0.4327 in normalized units. In the case of more than one magnetic component present in the core (usual case), the sum of the hb curves will apply.

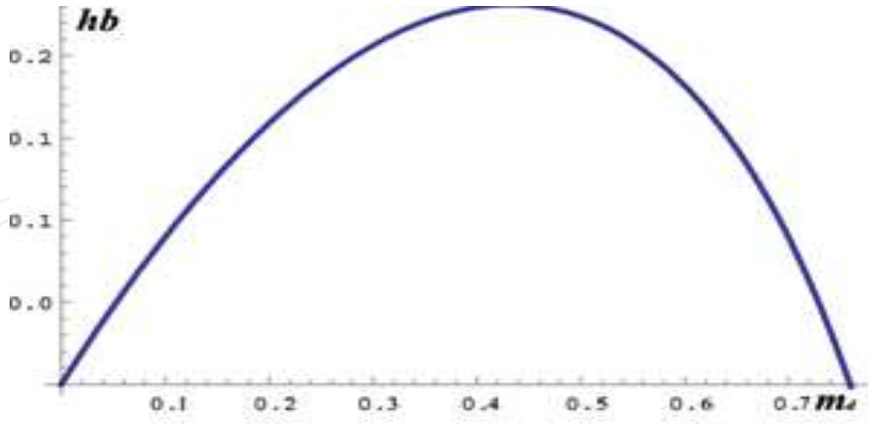

Fig. 10. Typical energy product as a function of induction.

6. Barkhausen jump and instability

Weiss postulated the domain structure for magnetic materials in 1907 but not until only 1919 was the existence of the ferromagnetic domains experimentally (Barkhausen, 1919) verified. In that year Barkhausen put a secondary coil around the specimen, under investigation and

connected it to an amplifier with a loudspeaker connected to its output. By Faraday's law the induced voltage in the coil is proportional to the rate of change of the induced flux. As the magnetic field was smoothly changed up or down at a constant rate, a series of pulses was heard on the loudspeaker, indicating, that a series of jumps were taking place in the magnetization process. That was the first verification that a magnetic substance is not composed of molecular size components but larger regions, called domains. The series of clicks indicated the movement, the size change or rotation of these domains. The continuous looking magnetization curve obtained experimentally is composed of a number of small jumps, or many small discontinuous flux changes. These jumps have an unpredictable random nature in space and time. The jumps represent an instant change in the microscopic magnetic state of the material. The system abruptly leaves a higher energy state for a lower one. Although it is random, its statistical average is characteristic to the material and is correlated with the previous magnetization or demagnetization period. These clicks are called Barkhausen jumps and the phenomenon is the Barkhausen effect or Barkhausen instability.

The mathematical description of the phenomenon proved extremely difficult. After several unsuccessful attempts recently Bertotti developed a comprehensive model based on stochastic principles. Although with one assumed statistical state, a large number of real domain structures can be associated, the calculated results of this model are so far in good agreement with experimental observations. For further details and wider discussion on the Barkhausen effect, the reader is referred to the literature (Bertotti, 1998).

Until now we have concentrated on the microscopic nature of the Barkhausen jump but the question arises whether similar jumps could occur at macroscopic level.

Let us look at equation (28), which shows the formula with a character of a feedback amplifier. It is obvious that, when the Weiss coefficient is a certain value the denominator goes to zero and the equation shows, that instability sets in the circuit. Expression (28) is independently applicable to any functions; therefore it is valid for (12) and (13) as well.

By introducing Weiss effective field, as defined in (25), into (12) and (13), they become:

$$m_u = a\ tanh[\alpha(h - h_c) + \beta m_u] + f_0(h_m) \tag{39}$$

$$m_d = a\ tanh[\alpha(h + h_c) + \beta m_d] - f_0(h_m) \tag{40}$$

$$f_0(h_m) = (m_u + m_d)/2 \text{ for h = h}_\text{m} \tag{41}$$

here β is the Weiss coefficient. From the equations above m_u or m_d cannot be expressed in closed mathematical form. Instead we express h as the function of $m_{u,d}$ and we obtain the following:

$$h_u = \frac{\textbf{arctanh}(\frac{m_u - f_0(h_m)}{a}) - \beta m_u}{\alpha} + h_c \tag{42}$$

$$h_d = \frac{\textbf{arctanh}(\frac{m_d - f_0(h_m)}{a}) - \beta m_d}{\alpha} - h_c \tag{43}$$

We can parametric plot these two expressions m_u and m_d as a function of h and from this graphical solution (Takacs, 2003), by using available computer technology, we can investigate graphically the behavior of m_u and m_d due to the variation in Weiss coefficient.

At values of $\beta < 1$ The angle of intersection between the major loop and the horizontal axis is less than a right angle. At $\beta = 1$ the intersection is 90^0. At $\beta > 1$, Barkhausen jump occurs in the hysteresis curve, between the two magnetization values, which belong to the same excitation field values. Fig. 11 shows the coexistence of the states simultaneously with two free energy values. Here the system can freely move between the two energy states (see later). The system jumps into a lower energy state (Bertotti, 1998) and this energy jump results in a loop similar to a hysteresis loop but the loop intersection with the horizontal axis is governed by the magnitude of β as shown in Fig. 11. On the example the jump occurs at the values of $m = \mp 0.70613$ and $h = \pm 1.0308$ as marked on Fig. 11. Starting with a demagnetized sample, beyond the critical value of β, when the first jump occurs, the sample cannot be demagnetized by any ac signal. For detailed explanation of the macroscopic Barkhausen jump and its effect on magnetization, the reader is referred to the literature (Della Torre, 1999). The shape of the loop is representative of the energy state of the system.

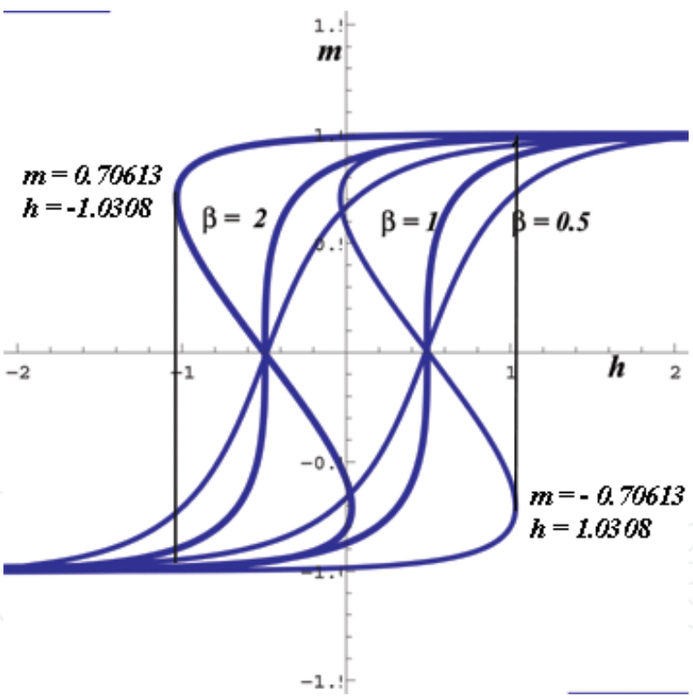

Fig. 11. Schematic hysteresis loops calculated from (42) and (43) showing the Barkhausen jump on macroscopic scales, β as parameter. Curves are for β = 0.5, 1 and 2 in arbitrary units.

In the following we are going to discuss the important relationship between system stability and the bistable system represented by the system with positive feedback.

Let us consider a system, where the m moment can freely move around under the influence of H external excitation (for the theoretical or intrinsic concept see Part 4) field. Then the

energy E of m_i moment without any hindrance from the interaction between the moments can be written as:

$$E = -\mu_0 H \sum_i m_i \tag{44}$$

According to Weiss' theory however the interaction between domains introduces an additional field as we see in Section 4 equ. (25), opposing the external magnetizing field. This internal field has an additional energy contribution in the following form:

$$E_{add} = -\frac{N_D}{2}\mu_0 \sum_{i,j} m_i m_j = -\frac{N_D}{2}\mu_0 M^2 \tag{45}$$

The energy resulting from effective field (see Section 4) of a magnetic moment can be written as:

$$E_i = -\mu_0 m_i H_{eff} + \frac{N_D}{2}\mu_0 M^2 \tag{46}$$

Based on the law of statistical mechanics and resulting from averaging process, the partition function of the system defined as:

$$Q_i = \exp(-\frac{1}{k_b T} E_i(m)) + \exp(-\frac{1}{k_b T} E_i(-m)) \tag{47}$$

By substituting Equ. 46 into (47) and using known mathematical relations we come to the following formulation:

$$Q_i = 2\exp(\frac{N_D \mu_0}{2k_b T} M^2)\cosh\frac{\mu_0 m_i}{k_b T} H_{eff} \tag{48}$$

Per definition the total free energy of N number of moments in a unity volume can be written as:

$$A = -k_b \sum_i^N \ln Q_i = \sum_i^N -\frac{N_D \mu_0}{2} m_i M + k_b T \ln(2\cosh\frac{\mu_0 m_i}{k_b T} H_{eff}) \tag{49}$$

After summation and some simplification we come to the following form

$$A = -\frac{N_D \mu_0}{2} m_i M + k_b T N \ln(2\cosh\frac{\mu_0 m_i}{k_b T}(H + \frac{N_D}{2} M) \tag{50}$$

Dividing (50) by $k_b T_c N_D$ where T_c is the Curie temperature defined as:

$$T_c = \frac{\mu_0 m M_m N_D}{2k_b} \tag{51}$$

and M_m is the maximum magnetization and with the material constant of b_0 representative of the magnetic properties of the sample under test

$$b_0 = \frac{N_D \mu_0 M_m^2}{2 k_b T_c N} \tag{52}$$

The normalized form of the Gibbs free energy for the up and down going branch of the hysteresis loop will be given in form of Equ.53 and 54 respectively

$$a_{u,free} = \ln[2\cos(h - n_d m_u)] + b_0 m_u \tag{53}$$

$$a_{d,free} = \ln[2\cos(h + n_d m_d)] - b_0 m_d \tag{54}$$

In Fig. 12 the free energy changes are shown for the up and down going branch of the hysteresis loop as the function of maximum magnetization, the parameter is the coercivity in arbitrary units.

Figs. 12 a and b clearly show the identical energy states, which belong to two different magnetization conditions, where the system can move freely between the two energy states. The system then moves to the lower energy state satisfying the laws of thermodynamics.

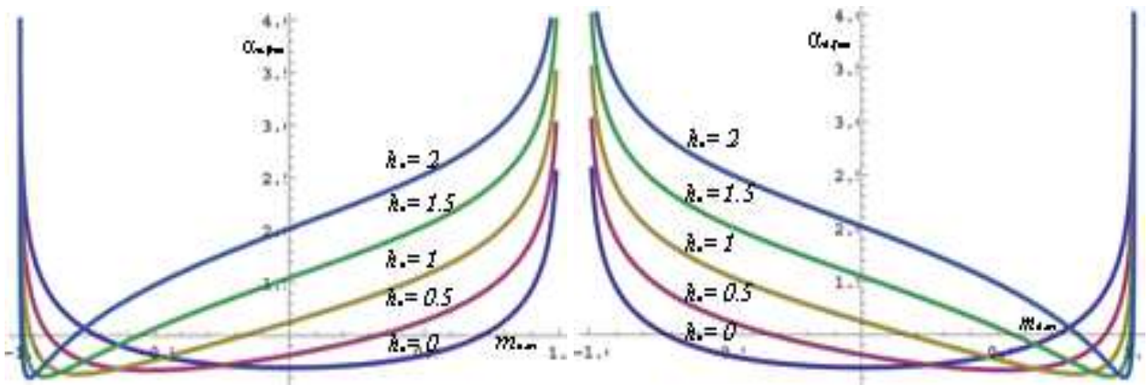

(a) (b)

Fig. 12. Gibbs free energy as the function of maximum magnetization. The parameter is the coercivity, in arbitrary units.

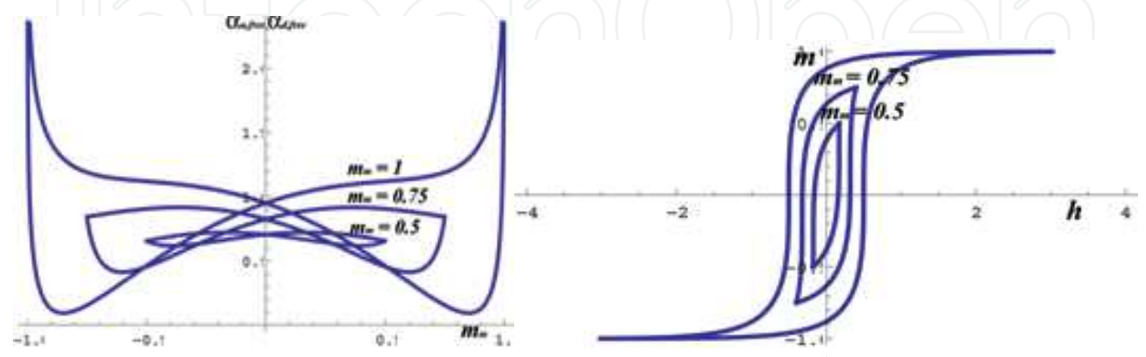

(a) (b)

Fig. 13. The free energy flow for major and minor hysteresis loops (a) Figure (b) shows the corresponding major and minor loops.

These are representing the points where the Barkhausen macroscopic instability can occur, when a positive $\beta > 1$ value creates a positive feedback.

We have to note, that during this calculation the effect of the temperature was neglected. We have assumed that the sample, under investigation, was kept around normal room temperature, well below the critical Curie point (see above). For further studies of the subject and for the impact of the temperature on the magnetization process, we refer the reader to the literature (Takacs, 2005; Bertotti, 1998). We did not feel that the temperature dependence fits into the framework of this study.

7. Eddy current loss

The hysteretic loss is by no means the only one that a magnetic substance suffers from, during magnetization. Most magnetic materials, in practical applications, (power transformers, relays etc.), are subjected to ac magnetization or the combination of both ac and dc fields. Fields, if they are not changing extremely slowly in time (quasi-static or rate independent) will alter the shape of the hysteresis loop due to the countering effect of the induced field in the magnetic medium, reducing the effectiveness of the applied external excitation. This phenomenon separates the rate independent or static hysteresis from the rate dependent hysteresis behavior. The magnetization process becomes a function of time and space. The mathematical treatment of the phenomenon is not easy, due to the fact that this phenomenon is strongly dependent on the shape of the sample and more other factors contribute to the loss. Eddy current losses depend on the conductivity of the magnetic substance and the size and shape of the magnetic circuit i.e. transformer. The analysis is further complicated by the inhomogeneity of the magnetic material used in practical applications. The theoretical treatment of these losses is difficult primarily because at no time can the sample be regarded as an infinite continuum, with homogeneous magnetic properties even when we neglect of the effect of the shape and the un-reproducible conductivity, which depends also on the previous treatment of the magnetic substance. The application of Maxwell's equations, for calculating the losses, therefore is difficult. Shockley, Williams and Kittel (Williams et al 1950; Cullity, 1972) were the first to look at this rather complex problem theoretically. The best approach to losses was made recently by Bertotti (Bertotti, 1998) on statistical principles. He introduced the concept of separation of losses and gave a theoretical verification to the dependence of the shape of the hysteresis loop on the various loss contributory factors. He expressed the separated losses in the following form.

$$W = W_h + W_{ed} + W_{ex} \tag{55}$$

Here W, the energy loss per cycle is given by the sum of W_h hysteresis, W_{ed} eddy current and the W_{ex} excess losses. Here the W_h hysteresis loss is proportional to the area enclosed by the static hysteresis loop (Steinmetz law, see section 5), the W_{ed} is the function of the first time derivative of the magnetization and W_{ex} covers all the other losses not included in the first two categories. Our intention is not to cover the whole problem of losses, only to apply a hyperbolic solution to the Everett integral to demonstrate the effect of W_{ed} on the shape of the hysteresis loop. This will give an approximate idea for the practical user on the relative magnitude of the eddy current effect. The following calculation relates to one unit cube of

the magnetic sample and other effects will be disregarded. We assume that the eddy current effect is the dominating factor in the magnetic losses. All other losses are included in W_h and W_{ex} category, which are not regarded as part of this Section.

Let us use the Weiss effective field, to express the effect of the eddy current as specified in (27). We can write the magnetization as

$$m_u = a\ tanh[\alpha(h - h_c) - \beta\frac{dm_u}{dt}] + \frac{a}{2}\{\tanh[\alpha(h_m + h_c) + \beta\frac{dm_u(h_m)}{dt}] - \tanh[\alpha(h_m - h_c) + \beta\frac{dm_u(h_m)}{dt}]\} \tag{56}$$

$$m_d = a\ tanh[\alpha(h + h_c) + \beta\frac{dm_d}{dt}] - \frac{a}{2}\{\tanh[\alpha(h_m + h_c) + \beta\frac{dm_d(h_m)}{dt}] - \tanh[\alpha(h_m - h_c) + \beta\frac{dm_d(h_m)}{dt}]\} \tag{57}$$

where β represents the eddy current loss factor and the additional field is proportional to the first time derivative of the magnetization.

The time derivatives of the magnetizations after using well known functional relations are

$$\frac{dm_u}{dt} = \frac{dm_u}{dh}\frac{dh}{dt} = a\alpha(1 - \frac{1}{a^2}m_u^2)\frac{dh}{dt} \tag{58}$$

$$\frac{dm_d}{dt} = \frac{dm_d}{dh}\frac{dh}{dt} = a\alpha(1 - \frac{1}{a^2}m_d^2)\frac{dh}{dt} \tag{59}$$

For triangular excitation, when T (not to be mistaken to the Preisach triangle or Tesla) is the duration of one period and ω is the repetition frequency

$$\frac{dm_u}{dt} = \frac{2h_m\omega}{\pi}a\alpha(1 - \frac{1}{a^2}m_u^2) \quad \text{for } -\frac{\pi}{2} < t < \frac{\pi}{2} \tag{60}$$

$$\frac{dm_d}{dt} = -\frac{2h_m\omega}{\pi}a\alpha(1 - \frac{1}{a^2}m_d^2) \quad \text{for } \frac{\pi}{2} > t > -\frac{\pi}{2} \tag{61}$$

Substitution of (58) and (59) into (56) and (57) respectively will give us the working expressions for the magnetization process, when the effect of eddy current is included in the calculation. In (56) and (57) we left out the already negligible second order terms in the calculations.

$$m_u = a\ tanh[\alpha(h - h_c) + \beta\frac{2h_m\omega}{\pi}a\alpha(1 - \frac{1}{a^2}m_u^2)] + \frac{a}{2}\{\tanh[\alpha(h_m + h_c) + \beta a\alpha\frac{2h_m\omega}{\pi}(1 - \frac{1}{a^2}m_u^2(h_m)] - \tanh[\alpha(h_m - h_c) + \beta a\alpha\frac{2h_m\omega}{\pi}(1 - \frac{1}{a^2}m_u^2(h_m)]\} \tag{62}$$

$$m_d = a\ tanh[\alpha(h-h_c)+\beta a\alpha\frac{2h_m\omega}{\pi}(1-\frac{1}{a^2}m_d^2)]$$
$$+\frac{a}{2}\{\tanh[\alpha(h_m+h_c)+\beta a\alpha\frac{2h_m\omega}{\pi}(1-\frac{1}{a^2}m_d^2(h_m)]- \quad (63)$$
$$-\tanh[\alpha(h_m-h_c)+\beta a\alpha\frac{2h_m\omega}{\pi}(1-\frac{1}{a^2}m_d^2(h_m)]\}$$

Fig. 14 shows the change in the shape of the hysteresis loop due to eddy current for β = 0, 0.1, 0.2, 0.3 and 0.4 loss factor, for an arbitrary hysteresis loop in arbitrary units. The losses are always proportional with the area enclosed by the hysteresis loop (Steinmetz law). In practical case therefore, the user need to know the static (dc) and the dynamic (ac) hysteresis loop area. The difference between the two is related to the total losses due to the ac magnetization. The eddy current loss is regarded as the dominant loss factor after the hysteretic loss.

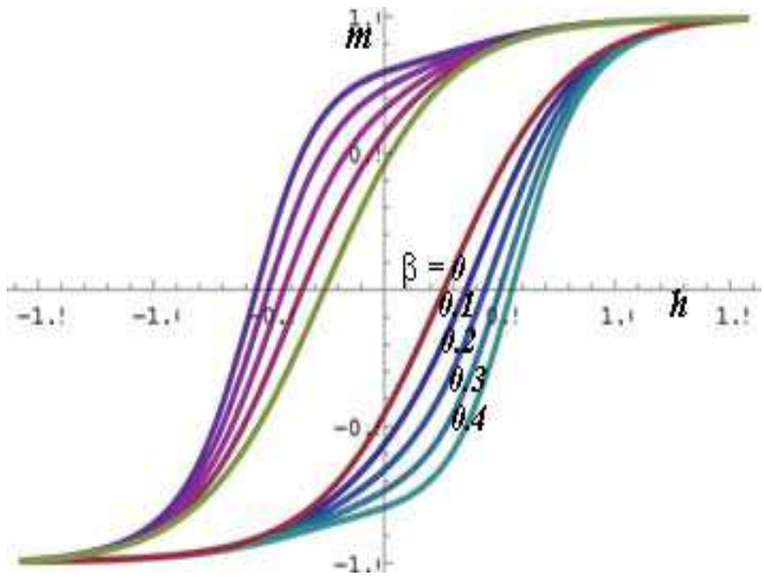

Fig. 14. Showing the effect of eddy current for β = *0,* 0.1, 0.2, 0.3 and 0.4 in arbitrary units.

For sinusoidal excitation the substitution is

$$h = h_m \sin\frac{T}{2\pi}\omega t \quad (64)$$

The excess losses are taken as the square root of the time derivative of the magnetization function. Its mathematical treatment is only possible in special cases. In most cases can only be handled by computerized numerical iteration.

The increase in area of the loop is proportional to energy loss in one period due to eddy current in an infinitely large sample of the modeled material. The frequency dependency of the eddy current loss can also be calculated from (62) and (63) without taking into account the frequency dependent skin effect. The penetration depth depends primarily on the conductivity of the material under test and the frequency used.

8. Coercivity and remanent magnetism

The coercive force is the magnetic field needed to reduce the magnetization level to zero. Generally, it is referred to as coercivity and it is one of the representative values of a ferromagnetic material. Its numerical value strongly depends of the pre-history of the sample, like mechanical treatment, temperature etc. It has a strong relationship with another characteristic parameter, i.e. the remanent magnetism at maximum magnetization, called remanence. As the field gradually reduced to zero, from positive saturation, the process, following the descending branch of the hysteresis loop, the magnetization recedes to this remanent magnetization value usually marked as M_r.

When the field gradually is reduced to zero from the positively saturated state ($h = h_m$), where $f_0 \sim 0$, the magnetization remains at a constant value, called remanence.

Fig. 15 depicts the measured and modelled remanence B_r as the function of the maximum excitation H_m for NO Fe-Si.

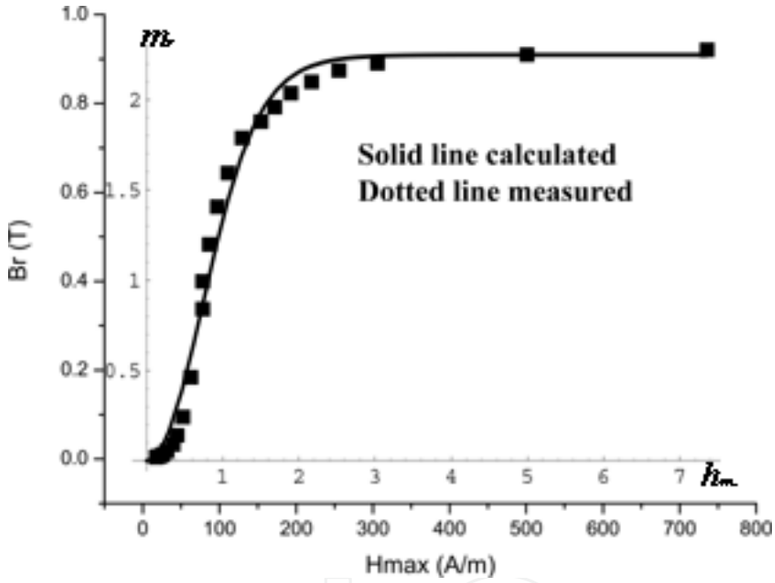

Fig. 15. Measured and calculated B_r remanence versus H_m maximum field excitation.

Take expression (13) and substitute $h = 0$. Expressing h_c we come to the mathematical relationship between coercivity (h_c) and remanence (m_r) in this form, for a single component.

$$h_c = \frac{1}{\alpha} \arctan \frac{m_r}{a} \tag{65}$$

This mathematical expression is valid for all major and minor loops.

By equating m with 0 in (16), the remanence can be calculated as the function of the maximum magnetizing field in the following form:

$$m_r = \sum_{k=1}^{n} [a_k \tanh\ \alpha_k h_{0k} - a_k \frac{\tanh\ \alpha_k h_{0k} - \tanh\ \alpha_k h_{0k} (\tanh\ \alpha_k h_m)^2}{1 - (\tanh\ \alpha_k h_{0k} \tanh\ \alpha_k h_m)^2}] \tag{66}$$

The total value of remanent magnetism is the sum of the remanence of the constituent components.

In Fig.16 a measured remanence curve for NO Fe-Si is shown with the modeled equivalent, calculated from (66).

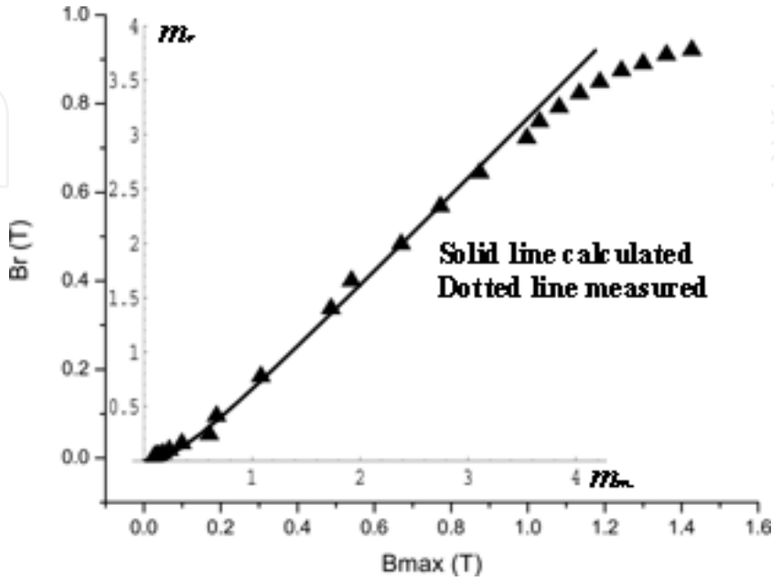

Fig. 16. Remanence versus maximum induction.

9. Spin valve and inverse spin valve character, negative coercivity

Magnetoresistive (MR) and Giant Magnetoresistive effects (GMR), the principles of spin valves, have been discovered in 1988. For many years it was only a scientific curiosity confined to research laboratories. The inverse spin valve, inverted variety of spin valve, based on similarity and not always associated with magnetism (Nemcsics et al. 2011), was discovered many years later. Today a large variety of sensors are based on these principles in vital industrial applications (Mallison, 2002).

Spin valve devices fundamentally consist of two ferromagnetic layers separated by a thin diamagnetic metal layer. One of the ferromagnetic layers, the so called reference layer is usually configured as an artificial anti-ferromagnet and pinned by exchange biasing to an anti-ferromagnetic layer. The other ferromagnetic layers (free layers) can freely change their magnetization direction under the influence of an external magnetic field (Jedlicska et al. 2010). Their $M = f(H)$ response characterized by the so called wasp-waisted loop shape. Its character show two interlinked hysteresis loops representing the switching of individual layers constituting the spin valve structure.

Fig. 17 depicts a typical characteristic spin valve, coupled double hysteresis loop. To our knowledge none of the hysteresis models can simulate any of these complicated structures. The hyperbolic model, with its flexibility and adaptability can model intricate and sophisticated structures, which are getting more popular in industrial applications. The model applications are not restricted to simple investigations of material parameters, but

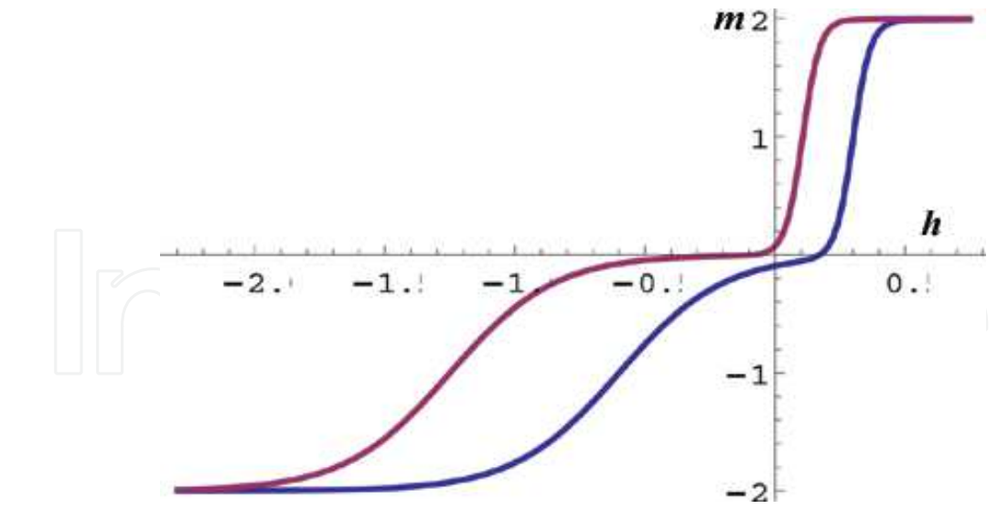

Fig. 17. Typical spin valve coupled hysteresis loops in arbitrary units.

can be applied to modeling instrument characteristic behavior and for the calculation of characteristic parameters of instruments.

Associated with the Magnetoresisrtive (MR) and Giant Magnetoresistive effects (GMR) is the phenomenon of negative coercivity in the hysteresis loop, which leads to three- looped hysteretic processes. This is due to the presence of the anti-ferromagnetic layer, forming part of the composite loop. By using (15), (16) and (17) for $n = 2$ and substituting negative numerical values for h_{c2} (anti-ferrous) we can model the overall character, where h_{cm} final coercivity changes from h_{cm} positive to $h_{cm} = 0$ and h_{cm} negative as shown in Fig. 18.

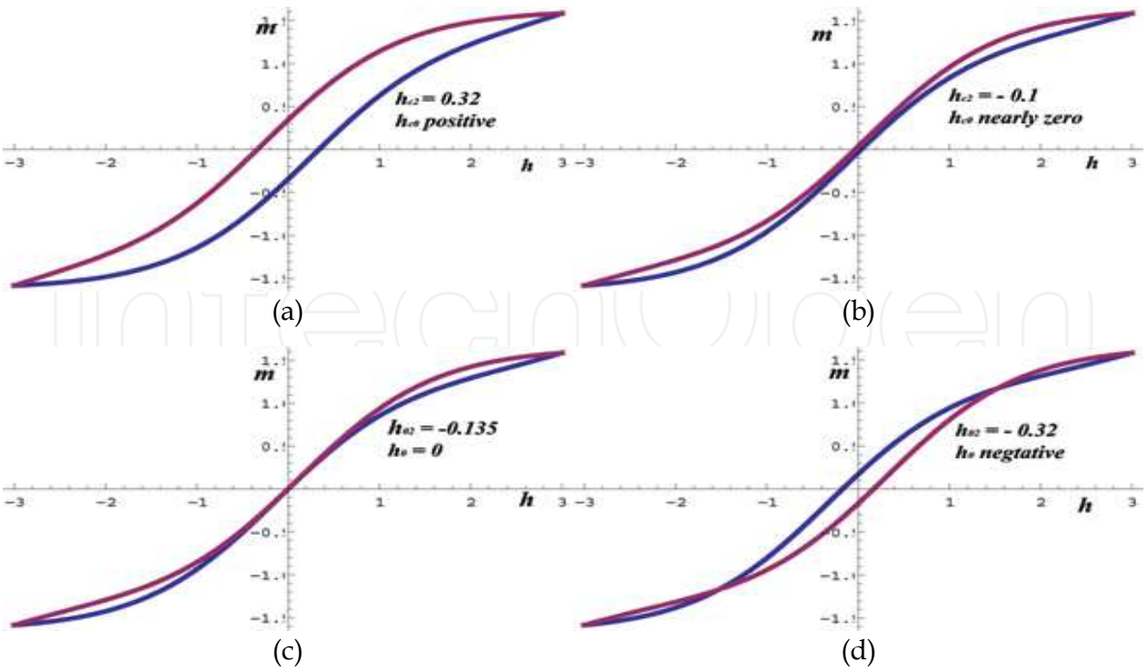

Fig. 18. h_{c0} at various values of h_{c2} a. Positive h_{20} b. Small negative h_{20} c. Medium negative h_{20} d. Larger negative h_{20}

The phenomena of hysteresis are not confined to magnetism. In other branches of the sciences like biology and semiconductor physics it is very common. Here, however we will demonstrate, what the model is capable of, not on a simple hysteresis loop, but on an inverse spin valve like loop, picked from the field of semiconductor surface physics. In Fig. 19 a RHEED specular spot intensity versus temperature diagram and its modelled curve is shown, which manifests itself in this complicated inverse spin like manner.

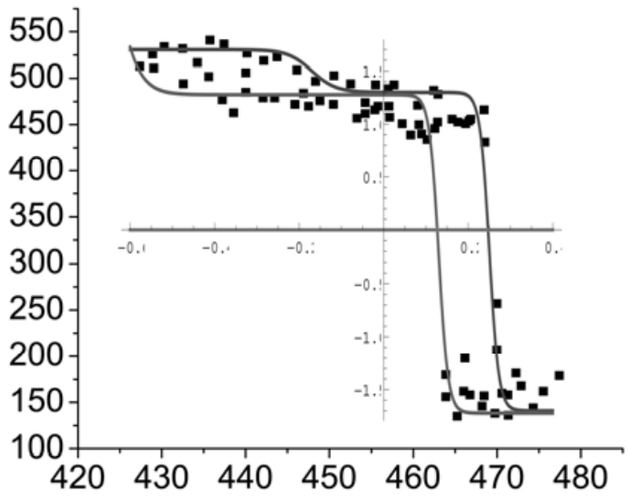

Fig. 19. An inverse spin valve character example from surface physics in arbitrary units.

10. Conclusion, process of identification, iteration, normalization and other practicalities

The hysteretic approach described here, based on Preisach model has a number of advantages. The most relevant once are:

a. The defining parameters can be the usual quantities used in practice: The maximum magnetization, coercivity, initial differential permeability (inclination). There are three in the simplest case (A, H_c, α). All tabulated in catalogues (Jiles, 1998)
b. The analytical relation between magnetization and field is a "soft" function, easy for mathematical operations (like integration). This is opposite of the Gaussian and Lorentzian approximations, which result in the error function and the inverse tangent functions, both are "hard " functions (Della Torre, 1999)
c. The hyperbolic approach does not suffer from the congruency restriction and correctly describes the minor loops between identical limits (Takacs, 2003)
d. The hysteron in the hyperbolic system retains its square like character, although it is hyperbolic in mathematical terms
e. All parameters are analytically identifiable from the major loop (Varga et al. 2008).

The hyperbolic model has its easy applicability in practical cases and has high accuracy as demonstrated on the practical examples. It has been shown, starting on biased minor loops, plus followed by hysteretic losses and other examples. The Barkhausen macroscopic jump

analytical approach has been done here for the first time, to our knowledge. An extra section is devoted to the internal demagnetization, which forced researchers to modify all other simple models, including that of CPSM. Here a model-independent mathematical approach is given to resolve this problem in a form, which is applicable to all simple models.

At the start the iteration in the curve fitting exercise to model the hysteresis curve from the experimental data the reader needs a set of initial or starting parameters. This is the first step in the identification process. In the simplest case this parameter number is three, which grows to nine for the most complicated composite material. a_0 is the amplitude of the maximum measured magnetization. When, more than one process is present, then $\sum_n a_k = a_0$. The ratio between the h_m and the starting value of coercitivity h_c is the same as that of the experimental data. The relation between coercivity and remanence is set by (63). The starting value for α can easily read from the measured data. With the appropriately selected initial set of data the iteration for fitting the experimental curve is converging whether the iteration is assisted by the computer software or purely carried out by manual process.

Most researchers normalize to the maximum values of the parameters. For instance, the magnetization is divided with M_m to get unity value for the normalized maximum magnetization. This however is not always an advantage.

Normalization is to help the user with the very often complicated mathematics and numerical calculations and must not be restricted to a single value like the maximum amplitude. Often is more convenient to choose other values or use free normalization, where the normalization base is only determined after the successful iteration, giving free hand to the user. Iteration can be based on the free transform facility, available in most graphic and Photo oriented software. The iteration can be carried out by using Mathematica, Mathlab, Origin or a number of other mathematical packages and it can be computer assisted or entirely manually interactive. The measured data and the calculated results should be saved in identical formatting such as PDF, EPS, JPEG, TIFF or others. When the calculated hysteresis loop or curve is reached a certain stage in similarity, it should be compared with the measured one, which can be stored in an appropriate formatting in transparent form (see Fig.20). The modeled loop should be copied then onto the measured data and stretched over the measured loop (conform transformation), as it is depicted in Fig. 21. Then one can see how much the parameter values need to be changed to make a closer fit to the experimental data. This iteration process will be repeated several times, until the experimenter is satisfied with the fit between the modeled and the experimental data either visually or numerically. When the iteration is finished and the experimenter is satisfied with the fit, the normalization for the final parameter values can be read from the two coordinate (measured and modeled) systems with the equivalent values on the scales (see Fig 21). Often the best approach is to start with manual iteration (human mind can make shortcuts). The final, tedious fine tuning can be left to the computer for time saving. Optimization packages used for optimization processes, like Genetic algorithm (GA) (Leite et al. 2004), Direct search (DS) (Kolda et al. 2003), Particle Swarm Optimization (PSO) (Marion et al. 2008), Differential Evolution (DE) (Toman et al. 2008) and others, have already been applied in similar iterative applications.

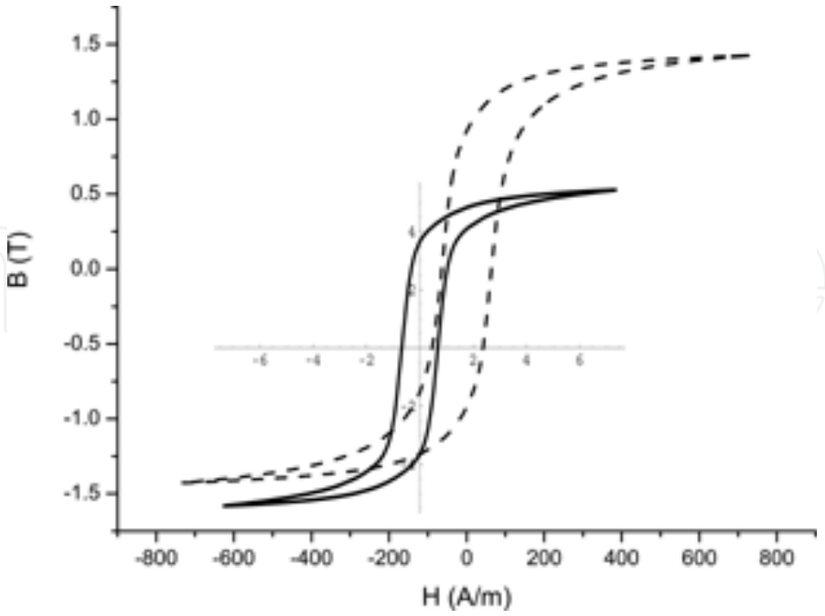

Fig. 20. Calculated (solid) loop is copied over the measured (dotted) curve in transparent mode.

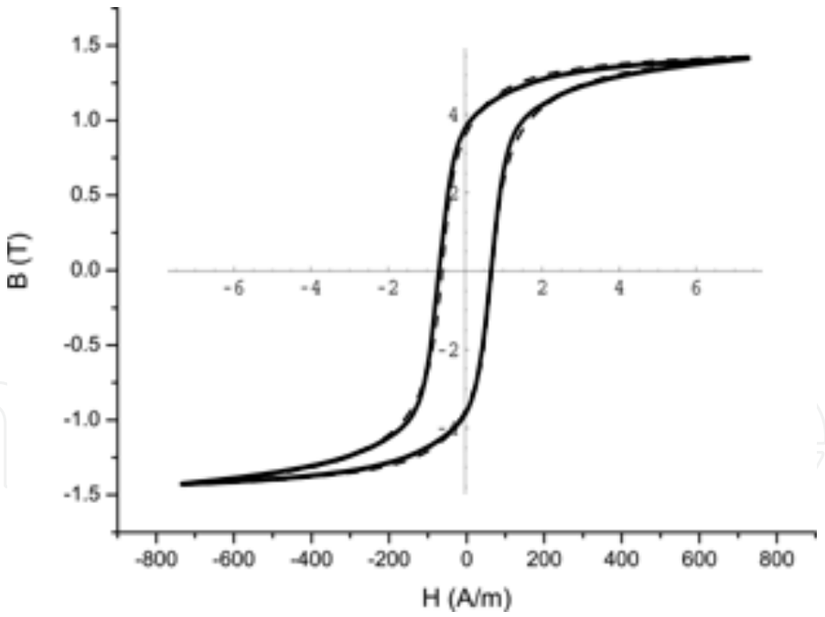

Fig. 21. The calculated loop is stretched over the experimental one

The number of calculations in the proposal is directed to the practitioner, who is interested in quick, easily achievable accurate results. Practical suggestions are included to help the potential users and encourage the model penetration into general engineering and other practices for fast and accurate modeling of large variation of magnetic materials used in industry and other fields of science.

11. Acknowledgement

I am grateful to I. Jedlicska, Gy Kovacs, L.K. Varga and R. Weiss for providing some of the experimental data for this contribution.

12. References

Alessandro B., Beatrice C. Bertotti G. and Montorsi A. (1990), pp. 2901 *J. Appl. Phys.* Vol. 68.
Barkhausen H. (1919), pp.(401) *Phyz. Z*. Vol. 29.,
Bertotti G. (1998) *Hysteresis in Magnetism*, Academic Press, London,.
Carpenter K. H. (1991) pp. 4404 *IEEE, Trans. on Magn*., Vol. 27.
Carpenter K. H. and Warren S. (1992), pp. 2037, *IEEE Trans. on Magn*., Vol. 28.
Cullity B. D. (1972), *Introduction to Magnetic Materials*, Addison – Wesley, Reading Mass.
Della Torre E. (1999), *Magnetic hysteresis*. IEEE Press, New York.
Finocchio G., Carpentieri M, Cardelli E. and Azzerboni B., (2006), pp. 451 *JMMM*, 300.
Fiorillo F. (2004), *Measurement and characterization of magnetic materials*, Elsevier Academic Press, Oxford.
Harison R. G. (2009), pp. 1922 *IEEE Trans. Magn*. 45., 4.
Ivanyi A. (1997), *Hysteresis Models in electromagnetic Computation*. Akademiai Kiado, Budapest.
Jiles D. C. and Atherton D. I. (1983), pp. 2183 IE*EE Trans.on Magn*.,Vol. 19.
Jiles D. C. and Atherton D. I. (1986), pp. 48 , *JMMM*, Vol 61.
Jiles D. C. IEEE Trans. on Magn. (1994), pp. 4326, Vol. 30.
Jiles D. C. (1998), *Magnetism and Magnetic Materials*, Chapman and Hall, London.
Jedlicska I., Weiss R. and Weigel R. (2008), pp. 884, *IEEE Trans. on Ind. El*.
Jedlicska, I.; Weiss, R.; Weigel, R. (2010), pp. 1728, *IEEE Trans. on Ind. Electronics* 57, 5.
Kadar Gy., (1987), pp. 4013, *J. of Appl. Phys*. 61.
Kadar Gy. and Della Torre E. (1988), pp. 3001, *J. of Applied Phys*., 63.
Kadar Gy., Kisdi-Koszo, Kiss E. L. Potocky L., Zatroch M.and Della Torre E. (1989), pp. 3931 *IEEE Trans. on Magn*. 25.,.
Kolda T. G., Lewis M. R., and Torczon V. (2003), pp. 385, *SIAM Review*, Vol. 45., No. 3.
Korman C. E. and Mayergoyz I. D. (1994), pp. 4368, *IEEE Trans. on Magn*., Vol. 30.
Leite J. V., Avila S. L., Batistela N. J., Carpes W. P., N. Sadowski N., Kuo-Peng P. and Bastos J. P. A. (2004), pp. 888, *IEEE Trans. on Magn*. Vol. 40., No. 2.
Mallinson J. C. (2002) *Magneto-Resistive and Spin valve Heads*., A.P. N.Y
Marion R., Scorretti R., N. Siauve N., M. A. Raulett M. A. and L. Krahenbuhl L. (2008) pp. 894, *IEEE Trans. on Magn*. Vol. 44. No. 6.
Mayergoyz I. D., Adly A A. and Friedmam G., (1990), pp. 5373, *J. of Appl. Phys*. 67.
Mayergoyz I. D., (2003), *Mathematical Models of Hysteresis and their Applications*, Academic Press, Elsevier, New York.
Nemcsics A. and Takacs J., (2011), pp. 91, *Semiconductors* 45.
Stoner E. C. and Wohlfarth E. P., (1991), pp. 3475, *IEEE Trans. on Magn*. 27.
Pike C. R., Roberts A. P. and K. L. Verosub K. L., (1999), pp. 6660, *J. Appl. Phys*. 85.
Preisach F., (1935), pp. 227, *Phys. Z*. 94 .
Steinmetz C., (1891), pp. 261, *The Electrician*, Jan 2.
Steimetz C., (1892), pp. 3, *IEEE Transactions*, 9.
Takacs J., (2000), pp. 1002 *COMPEL*, 20, 4,.

Takacs J., (2003), *Mathematics of Hysteretic Phenomena*, Wiley-VCH, Wenheim.
Takacs J., (2005), pp. 220, *COMPEL*, 24, 1.
Takacs J., (2006), pp. 57, *Physica B*., 372.
Takacs J. and Meszaros I., (2008), pp. 3137, *Physica B*. 403.
Takacs J., Kovacs Gy. and Varga L. K., (2008), pp. e1016, *JMMM*, 320.
Toman M., Stumberger G. and Dolinar D., (2008), pp. 1098, *IEEE Trans. on Magn*., Vol. 44, No. 6.
Tranter C. J., (1971), *Advanced Level of Pure Mathematics*, E.U.P., London.
Varga L. K., Kovacs Gy. and Takacs J., (2008), pp. L26, *JMMM*, 320.
Varga L. K., Kovacs Gy. and Takacs J., (2008), pp. e814, *JMMM* 320.
Williams H. J., Shockley W. and Kittel C., (1950), pp. 1090, *Phys. Rev*. Vol. 80.

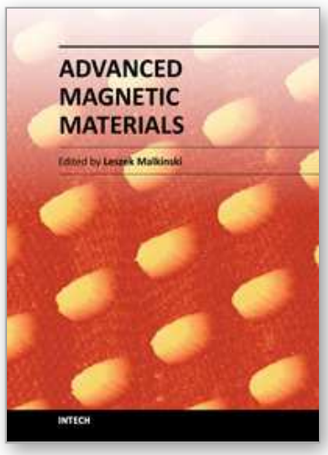

Advanced Magnetic Materials

Edited by Dr. Leszek Malkinski

ISBN 978-953-51-0637-1
Hard cover, 230 pages
Publisher InTech
Published online 24, May, 2012
Published in print edition May, 2012

This book reports on recent progress in emerging technologies, modern characterization methods, theory and applications of advanced magnetic materials. It covers broad spectrum of topics: technology and characterization of rapidly quenched nanowires for information technology; fabrication and properties of hexagonal ferrite films for microwave communication; surface reconstruction of magnetite for spintronics; synthesis of multiferroic composites for novel biomedical applications, optimization of electroplated inductors for microelectronic devices; theory of magnetism of Fe-Al alloys; and two advanced analytical approaches for modeling of magnetic materials using Everett integral and the inverse problem approach. This book is addressed to a diverse group of readers with general background in physics or materials science, but it can also benefit specialists in the field of magnetic materials.

How to reference

In order to correctly reference this scholarly work, feel free to copy and paste the following:

Jenõ Takács (2012). The Everett Integral and Its Analytical Approximation, Advanced Magnetic Materials, Dr. Leszek Malkinski (Ed.), ISBN: 978-953-51-0637-1, InTech, Available from: http://www.intechopen.com/books/advanced-magnetic-materials/the-everett-integral-and-its-analytic-approximation

INTECH
open science | open minds

InTech Europe
University Campus STeP Ri
Slavka Krautzeka 83/A
51000 Rijeka, Croatia
Phone: +385 (51) 770 447
Fax: +385 (51) 686 166
www.intechopen.com

InTech China
Unit 405, Office Block, Hotel Equatorial Shanghai
No.65, Yan An Road (West), Shanghai, 200040, China
中国上海市延安西路65号上海国际贵都大饭店办公楼405单元
Phone: +86-21-62489820
Fax: +86-21-62489821

IntechOpen